

The projection of a nonlocal mechanical system onto the irreversible generalized Langevin equation, II: Numerical simulations

Marc Vogt* and Rigoberto Hernandez†

Center for Computational and Molecular Science and Technology,
School of Chemistry and Biochemistry
Georgia Institute of Technology
Atlanta, GA 30332-0400

(Dated: November 19, 2018)

The irreversible generalized Langevin equation (iGLE) contains a nonstationary friction kernel that in certain limits reduces to the GLE with space-dependent friction. For more general forms of the friction kernel, the iGLE was previously shown to be the projection of a mechanical system with a time-dependent Hamiltonian. [R. Hernandez, *J. Chem. Phys.* **110**, 7701 (1999)] In the present work, the corresponding open Hamiltonian system is further explored. Numerical simulations of this mechanical system illustrate that the time dependence of the observed total energy and the correlations of the solvent force are in precise agreement with the projected iGLE.

I. INTRODUCTION

Several models for stochastic motion involve the Langevin and generalized Langevin equation (GLE) in so far as the environment is assumed to be in a steady-state equilibrium throughout the dynamical event, *vis-a-vis* the linear responding bath is stationary and obeys a fluctuation-dissipation theorem.^{1,2,3,4,5,6,7,8,9,10,11,12,13,14,15} In recent work,^{16,17,18,19,20} it was suggested that in many instances, the environment is not stationary, and as such a nonstationary version of the GLE would be desirable. In principle, it is easy to write a nonstationary GLE as

$$\dot{v} = - \int^t dt' \gamma(t, t') v(t') + \xi(t) + F(t), \quad (1a)$$

where $F(t) (\equiv -\nabla_q V(q(t)))$ is the external force, $v (= \dot{q})$ is the velocity, q is the mass-weighted position, $\xi(t)$ is the random force due to a solvent, and $\gamma(t, t')$ represents the nonstationary response of the solvent. To completely specify this system of equations, a closure connecting the random force to the friction kernel is needed. The fluctuation-dissipation relation (FDR) provides such a closure for the GLE.⁷ An obvious generalization of the FDR for nonstationary friction kernels is the requirement,

$$\gamma(t, t') = \langle \xi(t) \xi(t') \rangle. \quad (1b)$$

Unfortunately, such a construction will not necessarily be satisfied for an arbitrary nonstationary friction kernel, nor will it necessarily be associated with the dynamics of a larger mechanical system.

The GLE model with space-dependent friction (xGLE) developed by Lindenberg and coworkers,^{21,22} and Carmeli and Nitzan²³ does exhibit the structure of Eq. (1) and as such is an example of nonstationary stochastic dynamics. In recent work,^{16,17,18,19,20} a generalization of this model was developed which includes arbitrary nonstationary changes in the strength of the friction, but like the xGLE model does not include changes

in the response time. As such it is not quite the ultimately desired nonstationary GLE. Avoiding redundancy in the term “generalized GLE,” the new formalism has been labeled the *irreversible* generalized Langevin equation (iGLE), thereby emphasizing the irreversibility—vis-a-vis nonstationarity—in the response of the quasi-equilibrium environment. But this “irreversibility” may not persist at long times, and therefore Drozdov and Tucker chose to call such an equation of motion the multiple time-scale generalized Langevin equation (MTSGLE) in their application of the iGLE to study local density enhancements in supercritical fluids.²⁴

In this paper, the iGLE model is first summarized in Sec. II, explicitly indicating the limit in which position-dependent friction may be recovered. In earlier work,²⁰ (Paper I) it was shown that the iGLE may be obtained as a projection of an open Hamiltonian system, in analogy with the similar construction for the GLE.^{5,25,26,27,28} In Sec. II, the connections between the projection of the Hamiltonian of Paper I onto a chosen dynamical variable and that obtained by the xGLE are further illustrated, and the possibly troubling nonlocal term it contains is also further explored. The results of several numerical simulations of the Hamiltonian system are presented in Sec. III in order to illustrate the effect of the nonlocal term on the dynamics, and to verify that the constructed random force does obey the FDR.

II. THE iGLE AND SPACE-DEPENDENT FRICTION

A. Stochastic Dynamics

The iGLE may be written as

$$\dot{v}(t) = - \int_0^t dt' g(t) g(t') \gamma_0(t - t') v(t') + g(t) \xi_0(t) + F(t), \quad (2)$$

where $g(t)$ characterizes the irreversibility in the equilibrium environment, and there exists a FDR between the

Gaussian random force $\xi_0(t)$ and the stationary friction kernel $\gamma_0(t - t')$. Through the identities,

$$\gamma(t, t') \equiv g(t)g(t')\gamma_0(t - t') \quad (3a)$$

$$\xi(t) \equiv \xi_0(t), \quad (3b)$$

the iGLE is a construction of the nonstationary Eq. (1). One possible interpretation of the role of $g(t)$ in the iGLE is that it corresponds to the strength of the environmental response as the reactive system traverses the environment through an *a priori* specified trajectory, call it $y(t)$. Assuming that one also knows the field $f(y)$, which is the strength of the environmental friction over this configuration space, then the irreversibility may be written as,

$$g(t) = f(y(t)). \quad (4)$$

In the case that the chosen coordinate is itself the configuration space over which the friction varies —*i.e.*, $y = x$ — the GLE with space dependent friction of Carmeli and Nitzan is formally recovered.²³

But the iGLE is more general than the xGLE because it allows for a variety of “irreversible” time-dependent environments. For example, in the WiGLE model,¹⁹ each particle —labeled by n — is in an environment induced by the average of the properties of itself and w neighbors,

$$g_n(t) \equiv \langle |R(t)| \rangle_n^\zeta \quad (5a)$$

$$\langle |R(t)| \rangle_n \equiv \frac{1}{w+1} \sum_{i \in S_{w,n}} |R_i(t)|, \quad (5b)$$

where $S_{w,n}$ is the set of w neighbors. In the limit that $w \rightarrow 0$, the chosen coordinate is dissipated only by a function of its position, which is precisely the limit of space-dependent friction. In the limit that $w \rightarrow \infty$, the chosen coordinate is instead dissipated by a macroscopic average of the motion of all the reacting systems in the sample. The contribution of a particular particle to this average is infinitesimally small, and hence the friction contains no space-dependent friction. In between these limits, there is a balance between self-dissipation due to a space-dependent friction term, and heterogeneous dissipation due to the average of the motion of the w neighbors.

B. Mechanical Systems

In recent work, a Hamiltonian has been obtained whose projection is the iGLE when $g(t)$ depends exclusively on time —*i.e.*, it includes neither explicit space-dependence nor the WiGLE dependence.²⁰ This so-called

iGLE Hamiltonian may be written as

$$\begin{aligned} \mathcal{H}_{\text{iGLE}} = & \frac{1}{2}p_q^2 + \{V(q) + \delta V_1(q, t) + \delta V_2[q(\cdot), t]\} \\ & - g(t) \left[\sum_{i=1}^N c_i x_i \right] q \\ & + \sum_{i=1}^N \left[\frac{1}{2}p_i^2 + \frac{1}{2}\omega_i^2 x_i^2 \right], \end{aligned} \quad (6a)$$

where

$$\delta V_1(q, t) \equiv \frac{1}{2}g(t)^2 \sum_{i=1}^N \frac{c_i^2}{\omega_i^2} q^2 \quad (6b)$$

$$\begin{aligned} \delta V_2[q(\cdot), t] \equiv & \frac{1}{2} \int_0^t dt' a(t, t') [q(t') - q(t)]^2 \\ & - \frac{1}{2} \left[\int_0^t dt' a(t, t') \right] q(t)^2, \end{aligned} \quad (6c)$$

where

$$a(t, t') \equiv g(t)\dot{g}(t')\gamma_0(t - t'), \quad (7)$$

and the time dependence in $q(t)$ is explicitly included in the definition of the $\delta V_2[q(\cdot), t]$ functional for clarity. Ignoring the δV_2 term and identifying g as in Eq. (4), this Hamiltonian is similar to the xGLE Hamiltonian for space-dependent friction. This result is not surprising in the sense that the iGLE has a similar generalized structure. However, the xGLE Hamiltonian gives rise to an additional dependence on q whereas the iGLE Hamiltonian gives rise to an additional dependence on time t . The projections are thus analogous but not exactly the same.

C. Equation of Motion

The nonlocality in the $\delta V_2[q(\cdot), t]$ term does present some difficulties which are worth considering. In the absence of this term, the extremization of the action readily leads to the usual Hamilton’s equations. In general, the presence of the δV_2 term contributes to the time evolution of the momentum, \dot{p} , by what of the functional derivative,

$$-\frac{\delta S_2}{\delta q(t)}, \quad (8)$$

where the contribution to the action due to δV_2 may be written as

$$\begin{aligned} S_2 \equiv & \frac{1}{2} \int_0^T dt \int_0^t dt' a(t, t') q(t')^2 \\ & - \int_0^T dt \int_0^t dt' a(t, t') q(t) q(t'), \end{aligned} \quad (9)$$

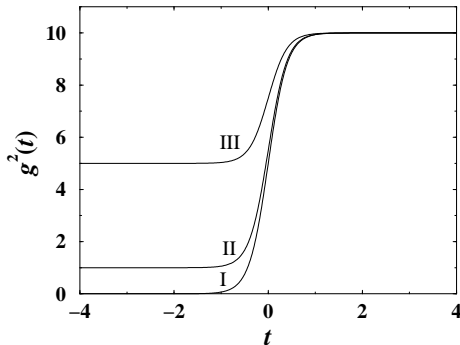


FIG. 1: The square of the irreversible change in the environment $g(t)^2$ is shown here as a function of time for the three cases examined in this study.

and T is the arbitrary final time to which the action is evaluated. A simple calculation readily leads to

$$-\frac{\delta S_2}{\delta q(t)} = \int_0^t dt' a(t, t') q(t') + \int_t^T dt' a(t, t') [q(t') - q(t)] . \quad (10)$$

The first time in the RHS precisely cancels the contribution due to the nonstationarity in the friction kernel. However, the remaining second term depends on the arbitrary final time T . It's presence can't be physically correct because it leads to different dynamics depending on the choice of T . In the limit that T is near—though greater—than t , this term vanishes, however. This suggests that an additional approximation ignoring the second term, thereby eliminating the transient effects from a term that depends arbitrarily on T , is warranted. (And this is consistent with the Carmeli and Nitzan derivation, in that they too need to remove transient terms.) Within this approximation, the projection in Ref. 20, then leads to the iGLE.

Thus the projection of the iGLE Hamiltonian leading to the iGLE with a purely time-dependent friction is analogous (& complementary) to the Carmeli & Nitzan projection to a GLE with space-dependent friction. The construction of such a Hamiltonian for an iGLE with arbitrary nonstationary friction, as manifested in WiGLE, is still an open problem. In the next section, the dynamics of the iGLE Hamiltonian is explored through numerical simulations in order to observe the degree of energy conservation—as it is affected by δV_2 —and the correlation of the constructed forces.

III. NUMERICAL RESULTS

In this section, numerical simulations of the Hamiltonian equivalent of the iGLE are presented. It is shown that the inclusion of the non-local term, $\delta V_2[q(\cdot), t]$,

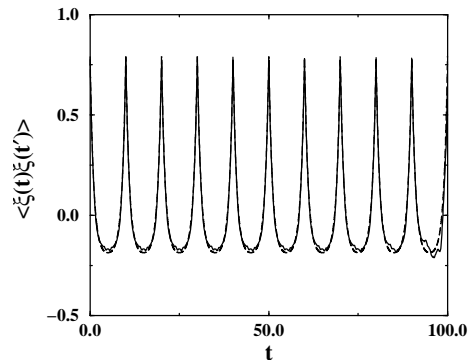


FIG. 2: The average correlation of the random forces on the tagged particle $\langle \xi(t)\xi(t') \rangle$ as a function of time t (solid line) for the GLE case with coupling constants calculated as in Eqn.tuckercrazy. The dashed line represents the friction kernel as calculated in Eqn.eq:freq.

known to be small in the quasi-equilibrium regime is actually necessary generally. That is, throughout this work, the value of $\delta V_2[q(\cdot), t]$ is non-zero during the increase in system coupling. The latter is specified through the function $g(t)$ chosen to satisfy

$$g(t)^2 = g(-\infty)^2 + \frac{1}{2}[g(\infty)^2 - g(-\infty)^2] \times \left(1 + \frac{e^{t/\tau_g} - 1}{e^{t/\tau_g} + 1}\right), \quad (11a)$$

as illustrated in Fig. 1, or equivalently as

$$g(t)^2 = \frac{1}{2}[g(\infty)^2 + g(-\infty)^2] + \frac{1}{2}[g(\infty)^2 - g(-\infty)^2] \tanh(t/\tau_g). \quad (11b)$$

A. Coupling Constants

The values of the coupling constants in Eqn. 6a can be obtained from the reverse cosine transform of Eqn. 13,

$$\frac{c_i^2}{\omega_i^2} = \frac{2\omega_c}{\pi} \int_0^\infty dt \cos(\omega_i t) \gamma_0 e^{-t/\tau}, \quad (12)$$

such that an effective (discretized) friction kernel of the form,

$$\gamma_0(t) = \sum_{i=1}^N \frac{c_i^2}{\omega_i^2} \cos(\omega_i t). \quad (13)$$

is used to approximate $\gamma_0 e^{-t/\tau}$. The coupling constants c_i in Eqn. 6a are readily obtained on a discrete (and finite) grid of N nontrivial frequencies, $\omega_i \equiv i\omega_c$, by equating the spectral densities of the exponential friction to that of discretization. The smallest frequency $\omega_c \equiv 1/(M\tau)$ can be characterized in terms of the characteristic integer M which effectively sets the longest time

scale that can be measured before false recurrences appear due to the discretization. The coefficients can be written (as, for example, also obtained by Topaler and Makri²⁹) as

$$c_i = \sqrt{\left(\frac{2\gamma_0\tau\omega_c}{\pi}\right) \cdot \left(\frac{\omega_i^2}{1 + \omega_i^2\tau^2}\right)}. \quad (14)$$

$1/(N\omega_c)$ represents the shortest time scale of interest. This connection between the continuum stationary friction kernel and the discrete number of frequencies and coupling strengths (Eq. 13) is exact in the continuum limit ($N \rightarrow \infty$). However, M must also be large enough so as to ensure the decay in correlations between the bath modes; typically $M \geq 4$. Simulations of the GLE (with constant friction) were performed to confirm a suitable number of bath particles for which convergence of the relationship in Eqn. 13 was observed. It was found that as few as 20 harmonic bath modes can yield acceptable convergence of the velocity correlation function of the chosen coordinate because its decay is much faster than the recurrence time in the bath modes. Nonetheless, to ensure that there are enough modes to approximately satisfy the continuum limit at the longest and shortest times of interest while also limiting the requisite computing power, the number of harmonic bath modes, N , used in the present work have been taken to be 200.

Although the coupling constants have been calculated as per Eq. 14 in the simulations of the mechanical projection of the iGLE presented in this work, it is beneficial to examine some other choices of the coupling constants, c_i . The main question is how to best equate the continuum (left hand side) and discrete (right hand side) representations of Eqn. 13 in the frequency domain. One alternative method is that of Tucker and coworkers,³⁰ in which the coupling constants are obtained, not by integrating the spectral function over an infinite domain as above, but over a domain bounded by the longest time scale $1/\omega'_c$. The resulting coefficients,

$$c_i = \sqrt{\left(\frac{2}{t_c}\omega_i^2\gamma_0\right) \left[\frac{1/\tau}{\omega_i^2 + 1/\tau^2} + \frac{e^{-t_c/\tau}\omega_i \sin(\omega_i t_c)}{\omega_i^2 + 1/\tau^2} \right]}, \quad (15)$$

are associated with a corresponding discrete frequency $\omega_i \equiv i\omega'_c$ as before, but the smallest frequency is redefined as $\omega'_c = \pi/(p\tau)$ for some characteristic integer p . The use of the coupling constants of Eq. 15 in the Hamiltonian representation of the GLE yields a very good match between the friction kernel as specified by Eqn. 13 and the correlation function for the random forces on the tagged particle as shown in Fig. 2. Unfortunately, the system still retains a long-time periodicity associated with the mode described by the largest inverse frequency. In an attempt to sidestep this issue, the chosen frequencies in the domain could be chosen incommensurably by choosing a frequency randomly within each window, $I_i \equiv (\{i-1\}\omega_c, i\omega_c]$. Given a random sequence of frequencies $\{\omega_i^R\}$ in which $\omega_i^R \in I_i$ for each i , the coefficients

can then be re-evaluated leading to the result,

$$c_i = \left\{ \left(\frac{2\gamma_0}{\pi}\right) (\omega_i^R)^2 \left[\tanh^{-1}(i\tau\omega_c) + \tanh^{-1}(\{i-1\}\tau\omega_c) \right] \right\}^{\frac{1}{2}}. \quad (16)$$

This choice of coefficients was also tested on the GLE but it led to similar results for the correlation function of the projected (random) forces $\xi(t)$, both in terms of the accuracy and in reproducing the long-time periodicity. It was therefore determined that the results for the GLE (and thereby the iGLE) are not highly sensitive to the limiting form of the coupling constants so long as the choice satisfies the appropriate friction kernel, while the random choice of frequencies did not remove the false long-time periodicity in the autocorrelation of the force $\xi(t)$.

This discussion, though somewhat pedantic, does offer a critical warning: any numerically measured behavior in the chosen particle that is correlated for times longer than the period of the false long-time periodicity in the discrete representation is suspect to error. This, in turn, places an upper bound on the slowest time scale — *viz.* t_g in Eq. 11 — that can be imposed on the nonstationary behavior of the bath coupling for a given choice of discrete oscillators in the Hamiltonian representation. In the simulations that follow, this bound is, indeed satisfied.

B. The Free Particle

The numerical equivalence between the iGLE and the Hamiltonian system of Eq. 6 can be illustrated using the same model of the nonequilibrium change in the environment originally investigated in the context of the phenomenological iGLE.¹⁶ To this end, numerical results are presented for the Hamiltonian system of a tagged free particle ($V(q) = 0$) bilinearly coupled to a bath of 200 harmonic modes whose smallest characteristic bath frequency is $\omega_c = 1/(M\tau)$ where $M = 4$. Individual bath frequencies are taken at discrete values, $\omega_i = (i-1/2)\omega_c$, and coefficients as per Eq. 14. All other parameters have identical values to those used in the numerical integration studies of the iGLE in Ref. 16 with the exception that 100,000 trajectories were used in this study, which is a 10-fold increase. In summary, all simulations share the following set of parameters: $N = 100,000$, $k_B T = 2.0$, $\gamma_0 = 10.0$, $\tau = 0.5$, $\tau_g = 0.2$, $\Delta t = 1 \times 10^{-4}$ ($t \geq -8$) and $\Delta t = 1 \times 10^{-3}$ ($t < -8$). The time dependent friction is modulated through the switching function $g(t)$ as shown in Fig. 1. Each individual trajectory is first equilibrated from $t = -20$ to ensure that the observed dynamics are influenced only by the irreversible change in the friction and not the dynamics of equilibration. The system is propagated using the velocity-Verlet method with

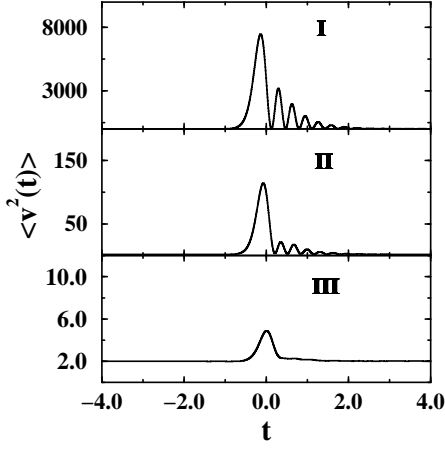


FIG. 3: The mean square velocity $\langle v^2(t) \rangle$ is displayed for each of the cases as a function of time t and case I, II or III with the non-local term $\delta V_2[q(\cdot), t]$ set equal to zero.

smaller timesteps during the regime of friction increase than for the constant friction regimes.³¹

In order to determine whether or not the $\delta V_2[q(\cdot), t]$ term is negligible, simulations were first performed with $\delta V_2[q(\cdot), t] = 0$. For all three cases of the change in friction, the non-local $\delta V_2[q(\cdot), t]$ term was found to be non-negligible as can be seen in Fig. 3 by the fact that the system does not obey equipartition of energy during times near $t = 0$. The larger the friction increase, the larger the deviation from equipartition. This can be seen in Fig. 3 as the largest deviations are seen for case I where the switching function $g(t)$ increases from 0 to 10. The friction increases along a similar range and the average square velocity $\langle v(t)^2 \rangle$ peaks at near 8000 around $t = 0$. The system does not conserve total energy in these cases.

However, upon introducing the nontrivial terms, $\delta V_2[q(\cdot), t]$ and its derivative (Eq. 6c), within the Hamiltonian equations of motion, equipartition for the system is preserved, as shown in Fig. 4. The $\delta V_2[q(\cdot), t]$ term is therefore not negligible in the extreme test cases examined in this work in which all the interesting time scales $1/\gamma_0$, t_g , and τ are comparable. Explicit integration of $\delta V_2[q(\cdot), t]$ is computationally expensive. This expense can be reduced when the stationary friction kernel has an exponential form. In this case, the derivative, $\frac{\partial \delta V_2[q(\cdot), t]}{\partial t}$, can be calculated using the auxiliary variable z , where

$$\frac{\partial z}{\partial t} = \dot{g}(t)q(t) - \frac{1}{\tau}z(t). \quad (17)$$

The value of $\frac{\partial \delta V_2[q(\cdot), t]}{\partial t}$ can then be obtained at each timestep,

$$\frac{\partial \delta V_2[q(\cdot), t]}{\partial t} = \gamma_0 g(t)z(t). \quad (18)$$

All of the results shown in this paper have been calculated using the integration of the auxiliary variable z because

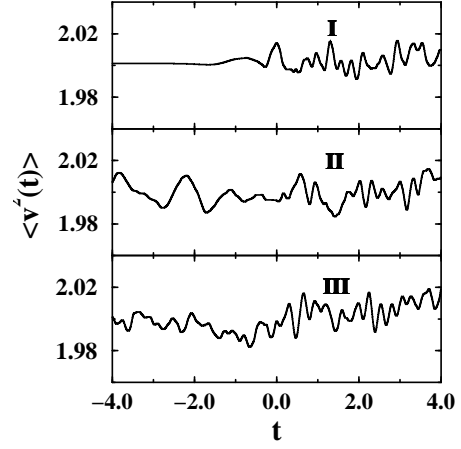


FIG. 4: The mean square velocity $\langle v^2(t) \rangle$ is displayed for each of the cases as a function of time t and case I, II or III with the non-local term $\delta V_2[q(\cdot), t]$ explicitly considered.

it is consequently formally equivalent to the explicit integration of Eq. 6c while requiring fewer computing cycles.

As can be seen from Fig. 4, all three test cases lead to the same level of fluctuations in the long time regime even though they begin from different initial states. In the limit of an infinite number of trajectories, all cases would exhibit no fluctuations, but these fluctuations due to finite size effects are indicative of the system dynamics. For example, in case I the particle obeys equipartition perfectly for the early regime, because its motion is ballistic, whereas the early time dynamics for cases II and III clearly show the influence of coupling to the harmonic bath particles. It can be seen from the plot of the average square velocity that the system conserves energy in these calculations when the $\delta V_2[q(\cdot), t]$ term is included. Unfortunately the additional test for the conservation of energy cannot be computed directly in these cases because $\delta V_2[q(\cdot), t]$ depends on the function $q(t)$ which cannot be known *a priori*.

The construction of the iGLE also requires that the correlation function of the random forces satisfies a non-stationary extension of the FDR,

$$k_B T g(t)g(t')\gamma_0(t-t') = \langle \xi(t)\xi(t') \rangle, \quad (19)$$

with respect to the explicit forces $\xi(t)$ on the tagged particle seen in a microscopic system,

$$\xi(t) = \dot{v} + \gamma_0 g(t) \int_0^t dt' g(t')\gamma_0(t-t')v(t') - F(t). \quad (20)$$

That the mechanical system satisfies this relationship is illustrated in Fig. 5, Fig. 6 and Fig. 7 for cases I, II and II respectively. The integral can be simplified using an auxiliary variable z_2 akin to the method for replacing $\delta V_2[q(\cdot), t]$ with z . The auxiliary variable satisfies,

$$\frac{\partial z_2}{\partial t} = \dot{g}(t)v(t) - \frac{1}{\tau}z_2(t). \quad (21)$$

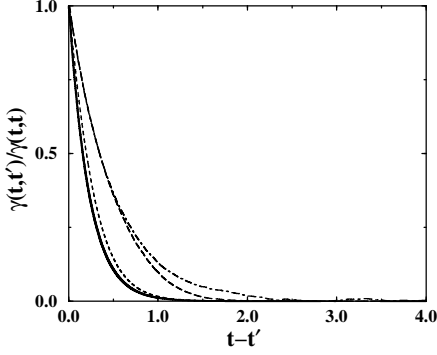


FIG. 5: The nonstationary friction kernel $\gamma(t, t')$ in case I at several different times t (-4.0 thick solid line, -0.5 solid line, 0.0 dashed line, 1.0 long dashed line and 4.0 dot dashed line) as a function of the previous times $t - t'$. The friction kernel is normalized by the value $\gamma(t, t)$ for illustrative and comparative purposes.

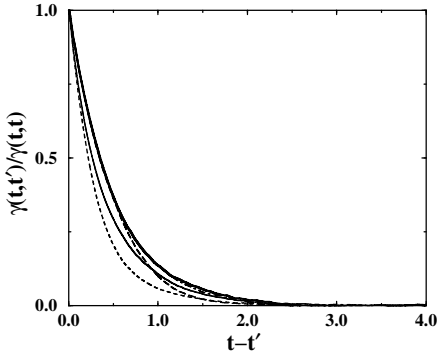


FIG. 6: The nonstationary friction kernel $\gamma(t, t')$ in case II at several different times t (-4.0 thick solid line, -0.5 solid line, 0.0 dashed line, 1.0 long dashed line and 4.0 dot dashed line) as a function of the previous times $t - t'$. The friction kernel is normalized by the value $\gamma(t, t)$ for illustrative and comparative purposes.

The explicit expression for the forces on the tagged particle can then be obtained at each timestep by substitution,

$$\xi(t) = \dot{v} + \gamma_0 g(t) z_2(t) - F(t). \quad (22)$$

The autocorrelation function of the force due to the bath —*viz.*, the random force in the projected variables— obey the FDR for all cases and times. It should be emphasized that this remarkable agreement would not have been found if the nonlocal term were omitted.

The velocity autocorrelation functions for the tagged free particle are shown in Fig. 8. The dynamics of the chosen coordinate changes in the same manner as for the studies on the numerical integration of the iGLE. The curves match the previous results exactly with the exception that the $t = 0$ and $t = -0.5$ were mislabeled in Ref. 16. The long time ($t = 4.0$) autocorrelation functions

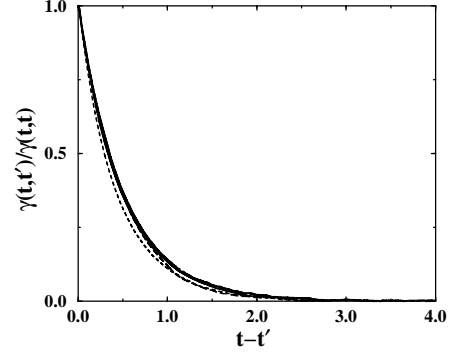


FIG. 7: The nonstationary friction kernel $\gamma(t, t')$ in case III at several different times t (-4.0 thick solid line, -0.5 solid line, 0.0 dashed line, 1.0 long dashed line and 4.0 dot dashed line) as a function of the previous times $t - t'$. The friction kernel is normalized by the value $\gamma(t, t)$ for illustrative and comparative purposes.

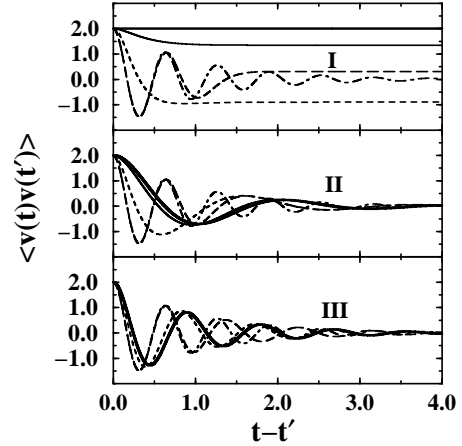


FIG. 8: The autocorrelation function of the velocity of the free tagged particle, $\langle v(t)v(t') \rangle$, is displayed for each of the three cases of the change in friction at initial times $t =$ (-4.0 thick solid line, -0.5 solid line, 0.0 dashed line, 1.0 long dashed line and 4.0 dot dashed line). The panels indicate cases I, II and III from top to bottom.

are all the same indicating that all cases reach the same equilibrium as would be expected. In case I, the early time ($t = -4.0$) autocorrelation function is a straight line since the particle is in the ballistic regime. All curves start at approximately 2.0 for $t - t' = 0$ since the system satisfies equipartition.

C. The Particle in a Harmonic Potential

The same simulations were run for a tagged particle in a harmonic well characterized by a frequency $\omega = 1$. The results are essentially all the same with the following exceptions: The system with tagged particle in a har-

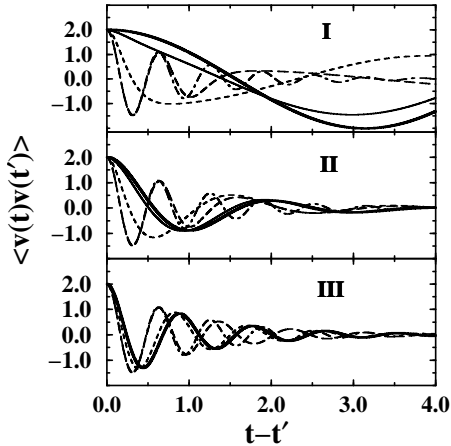


FIG. 9: The autocorrelation function of the velocity of the harmonic tagged particle, $\langle v(t)v(t') \rangle$, is displayed for each of the three cases of the change in friction at initial times $t =$ (-4.0 thick solid line, -0.5 solid line, 0.0 dashed line, 1.0 long dashed line and 4.0 dot dashed line). The panels indicate cases I, II and III from top to bottom.

monic well is less sensitive to the increase in friction and can be simulated accurately with larger timesteps than the free particle case due to the confining effect of the harmonic well. Similarly, the system does not yield such large spikes in the average square velocity for simulations with $\delta V_2[q(\cdot), t] = 0$, although the explicit calculation of that term is still a necessity for accurate results. Clearly the early time dynamics will differ between the free particle and harmonic particle cases as can be seen from the velocity autocorrelation functions for the harmonic tagged particle case in Fig. 9. Interestingly though, this is only the case for case I. In cases II and III the dynamics are essentially identical to the free particle case. This is due to the fact that the initial friction and thus the coupling is so strong (10.0 for case I and 50.0 for case

II) that the tagged particle potential has an insignificant contribution to the energy as compared to the contribution from the interaction with the bath.

IV. CONCLUDING REMARKS

The equivalence of the stochastic iGLE and the deterministic Hamiltonian system has been demonstrated by numerical integration of the equations of motion corresponding to the Hamiltonian in Eqn. 6a. The Hamiltonian system with 200 bath particles has been shown to exhibit equivalent dynamics as that seen in numerical integration of the iGLE. This is expected to be the case in the infinitely large bath size regime. The equivalence is contingent upon the explicit evaluation of the non-local dissipative term which is non-zero for all the cases of interest in this study. Although the free particle and harmonic oscillator cases do not contain a reactant/product boundary, they should be sufficient to verify the general agreement between the iGLE and the mechanical oscillator system. The deterministic mechanical system serves as further evidence that the stochastic equation of motion is not purely a fiction (e.g., phenomenological), but rather is equivalent to a physical system with an explicit energy function or Hamiltonian.

V. ACKNOWLEDGMENTS

We gratefully acknowledge Dr. Eli Hershkovitz for insightful discussions and Dr. Alexander Popov for a critical reading of the manuscript. This work has been partially supported by a National Science Foundation Grant, No. NSF 02-123320. The Center for Computational Science and Technology is supported through a Shared University Research (SUR) grant from IBM and Georgia Tech. Additionally, RH is the Goizueta Foundation Junior Professor.

* Present address: Department of Biochemistry and Molecular Biology, University of Massachusetts, 913 Lederle Graduate Research Tower, 710 North Pleasant Street, Amherst, MA 01003

† Author to whom correspondence should be addressed; Electronic address: hernandez@chemistry.gatech.edu.

¹ H. A. Kramers, *Physica (Utrecht)* **7**, 284 (1940).

² R. Zwanzig, *J. Chem. Phys.* **33**, 1338 (1960).

³ R. Zwanzig, *Statistical mechanics of irreversibility* (Wiley-Interscience, New York, 1961), vol. 3, pp. 106–141.

⁴ J. Prigogine and P. Resibois, *Physica* **27**, 629 (1961).

⁵ G. W. Ford, M. Kac, and P. Mazur, *J. Math. Phys.* **6**, 504 (1965).

⁶ H. Mori, *Prog. Theor. Phys.* **33**, 423 (1965).

⁷ R. Kubo, *Rep. Prog. Theor. Phys.* **29**, 255 (1966).

⁸ J. T. Hynes, *The theory of reactions in solution* (CRC,

Boca Raton, FL, 1985), vol. 4, pp. 171–234.

⁹ J. T. Hynes, *Annu. Rev. Phys. Chem.* **36**, 573 (1985).

¹⁰ A. Nitzan, *Adv. Chem. Phys.* **70**, 489 (1988).

¹¹ B. J. Berne, M. Borkovec, and J. E. Straub, *J. Phys. Chem.* **92**, 3711 (1988).

¹² P. Hänggi, P. Talkner, and M. Borkovec, *Rev. Mod. Phys.* **62**, 251 (1990), and references therein.

¹³ S. C. Tucker, M. E. Tuckerman, B. J. Berne, and E. Pollak, *J. Chem. Phys.* **95**, 5809 (1991).

¹⁴ S. C. Tucker, *J. Phys. Chem.* **97**, 1596 (1993).

¹⁵ E. Pollak, *Theory of activated rate processes* (Marcel Dekker, New York, 1996), pp. 617–669.

¹⁶ R. Hernandez and F. L. Somer, *J. Phys. Chem. B* **103**, 1064 (1999).

¹⁷ R. Hernandez and F. L. Somer, *J. Phys. Chem. B* **103**, 1070 (1999).

- ¹⁸ F. L. Somer and R. Hernandez, J. Phys. Chem. A **103**, 11004 (1999).
- ¹⁹ F. L. Somer and R. Hernandez, J. Phys. Chem. B **104**, 3456 (2000).
- ²⁰ R. Hernandez, J. Chem. Phys. **111**, 7701 (1999).
- ²¹ K. Lindenberg and V. Seshadri, Physica A **109A**, 483 (1981).
- ²² K. Lindenberg and E. Cortés, Physica A **126A**, 489 (1984).
- ²³ B. Carmeli and A. Nitzan, Chem. Phys. Lett. **102**, 517 (1983).
- ²⁴ A. N. Drozdov and S. C. Tucker, J. Phys. Chem. B **105**, 6675 (2001).
- ²⁵ R. Zwanzig, J. Stat. Phys. **9**, 215 (1973).
- ²⁶ A. O. Caldeira and A. J. Leggett, Phys. Rev. Lett. **46**, 211 (1981), Ann. Phys. (N. Y.) **149**, 374 (1983).
- ²⁷ E. Cortés, B. J. West, and K. Lindenberg, J. Chem. Phys. **82**, 2708 (1985).
- ²⁸ E. Pollak, J. Chem. Phys. **85**, 865 (1986).
- ²⁹ M. Topaler and N. Makri, J. Chem. Phys. **101**, 7500 (1994).
- ³⁰ S. Reese, S. Tucker, and G. Schenter, J. Chem. Phys. **102**, 104 (1995).
- ³¹ M. P. Allen and D. J. Tildesley, *Computer Simulations of Liquids* (Oxford, New York, 1987).

